Precise account of frictional loads in motor current-based compensation system of cutting force-induced error

G Turyagyenda*, **J Yang,** and **H Wu**
School of Power and Mechanical Engineering, Shanghai Jiaotong Univeristy, Shanghai, People's Republic of China

The manuscript was received on 26 March 2007 and was accepted after revision for publication on 05 July 2007.

DOI: 10.1243/09544062JMES678

Abstract: The balance between precision and its cost implications is a major determining factor for the competitiveness in the contemporary machining industry. The current paper presents an inexpensive compensation system for cutting force induced error based on current sensory system for indirect monitoring of cutting force. Based on machining parameters and online sensor signal, a dedicated model predicts the corresponding error. The model precisely accounts for the complex phenomena of coulomb and viscous frictions in the transmission system. Finally, the predicted error is compensated by means of external shifting of respective coordinate system origins in real-time. This system is convenient and reliable and, in addition, precise and easy to repair. The experimental evaluation of the system demonstrated robustness and great enhancement of machine accuracy.

Keywords: cutting force-induced error, error compensation, Coulombic friction, viscous friction, modelling

1 INTRODUCTION

Traditionally, machine errors are foreseen and avoided by means of careful design and manufacture through machine tool building process. The errors that survive through the careful design and manufacture are incorrectly assumed infinitesimal small and regrettably ignored. In the past time, machine builders assumed that careful design and manufacture produces ideal that, in turn, give perfect assemblies. It was further assumed that the accuracy status of machine tools is independent from influences of dynamics of machining processes.

On the contrary, actual workpieces produced are not as perfect as supposed and their accuracies are influenced by the dynamic conditions of the environmental and machining operations. This is indicative of the fact that careful design and manufacture does not completely avoid the machine inaccuracies particularly inaccuracies dependent on machine dynamics. As well, the cost of improving the machine accuracy increases exponential with increase in accuracy requirements [**1**]. Therefore, traditional means of improving machine accuracy by avoidance method is unreliable, complex, and comparatively extravagant. Based on this, the alternative of error compensation provides a more viable solution for improving accuracy in machine tools.

The origin of errors in machine tools is vast and complex, include quasi-static (geometric and thermal), cutting force-induced and other dynamic error components. Quasi-static errors are major causes of machine inaccuracies, hence in the past decades; research has focussed on theoretical modelling of geometric and thermal error components. Based on the study of geometrical errors [**2**], model has been developed and implemented for compensation of geometric errors on computer numerical controlled (CNC) machine tools. Similarly, quasi-static errors have been compensated by employing homogenous transformations [**3**] for representation of general volumetric error.

Although the quasi-static errors are dominating components of machine errors, after their

Corresponding author: School of Power and Mechanical Engineering, Shanghai Jiaotong University, 800 Dongchuan Road, Min Hang, Shanghai 200240, People's Republic of China. email: tgelvis@hotmail.com or twgelvis@yahoo.com

compensation, cutting force-induced errors becomes a principal source of machine inaccuracy. Since the productivity and economics of machining process is increasingly dependant of high precision, therefore among others cutting force-induced errors cannot be ignored. Research studies [**3**] have been carried out on the effects of cutting force onto machine tool accuracies. Theoretical models [**4**, **5**] for prediction of machining error induced by cutting forces have proposed. Among them, mechanistic modelling [**6**], based on cutting tool and machine tool parameters has been employed as means of determining of cutting forces.

Alternatively, current signals of drive motors have been monitoring as a means of indirectly predict of cutting force in machine tools [**7**]. Though economical and convenient, indirect monitoring systems have long control chains that introduce complex phenomena into the modelling process. Among these phenomena are coulomb and viscous frictional loads [**8**, **9**] inherent with the kinematic system of the machine tools. Also related application adaptive control [**10**, **11**] for cutting force has been developed aimed at regulation of cutting forces in machining processes.

The current paper presents a cutting force-induced error compensation system based on indirect monitoring cutting force. The cutting force is estimated using combination of hardware, modelling, and software tools. The correctness of the system is based on careful analysis and precise account of coulomb and viscous frictional loads with caution to the influence from load variations. To ensure precise results and cost-effectiveness systems, two parallel procedures were adopted each centred on force dynamometer and Hall effect sensor for data acquisition. Concurrently, deformations corresponding to cutting forces are acquired through a system of position sensor. Finally, the acquired data and machine parameters are analysed and the results are adopted for modelling and calibration of the online sensor.

2 EXPERIMENTAL STUDIES AND DATA ACQUISITION

The discrete variation of cutting force was achieved through a series of different depth of cut. A 10 mm-diameter tool tungsten carbide was used on carbon steel workpiece. Machining experiments were done at angular velocity of 1200 rpm and feed rate 3 mm/sec with a discrete variation for depth of cut of 0.04 mm. As shown in Fig. 1, cutting loads were directly and indirectly monitored by Kistler force dynamometer and Hall effect current sensors, respectively. Simultaneously inductive and magnetic position sensors are deployed together with force load monitoring systems for monitoring of the corresponding induced deformations. Finally, based on the data from force

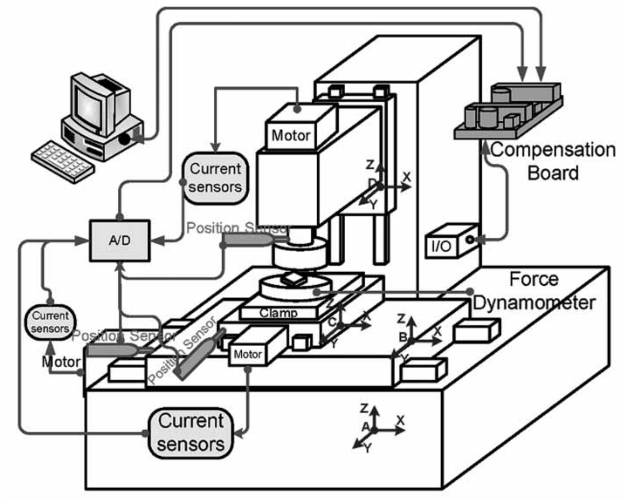

Fig. 1 Schematic of the experimental setup

dynamometer and position sensor, the online current sensors are comprehensively calibrated and the cutting force error prediction model developed.

Nevertheless, the cutting force exists in a complex amalgamation of coulomb and viscous frictional loads. Even more inconveniently, the frictional loads are further subdivided into load dependent and independent components.

In order to accurately determine each component of the complex entanglement, two strategic procedures are adopted. First procedure: cutting force is constrained to zero value while angular velocity is also constrained to discrete constant value to enable correctly isolate the load independent components of Coulombic and viscous friction. Second procedure: cutting forces are instead constrained to discrete (non-zero) constant values while angular velocity is also constrained to discrete constant value. Then, based on results from first procedure and also readings from force dynamometer and current sensors, the load-dependent components of coulombic and viscous frictional loads are determined. At the same time, the relationship between the cutting force and its induced errors are established based on the data provided by the positions sensors.

Considering the principle of conservation energy, a variation of cutting force in machine tools induces a variation of current of the drive motor. Therefore, the motor current is influenced by the variation of cutting force, indicating that by monitoring changes of motor current can be used to predict changes of cutting force.

Equilibrium of the dynamic influences on the system [**9**, **11**] equation is

$$J_{(\gamma)}\boldsymbol{\varepsilon}_{(\gamma)} = \boldsymbol{K}_{\mathrm{T}(\gamma)} \cdot I_{\mathrm{T}(\gamma)} - B_{(\gamma)} \cdot \boldsymbol{\omega}_{(\gamma)} - [\boldsymbol{T}_{\mathrm{Bf}(\gamma)} + (\boldsymbol{T}_{\mathrm{fl}(\gamma)} + \boldsymbol{T}_{\mathrm{fnl}(\gamma)}) + \boldsymbol{T}_{\mathrm{cf}(\gamma)}] \quad (1)$$

representing the relationship between cutting force, system inertia, and frictional loss components. Since the frictional, inertia, and cutting loads intermingled together in order to determine current and cutting force relationship, two strategic procedures are as follows.

Procedure 1. Six series of no-cutting experiments are run at discrete and constant angular velocities ($\boldsymbol{\omega}_{(\gamma)}$) for each of x, y, and z feed systems. Implying that cutting force torque ($\boldsymbol{T}_{\mathrm{cf}(\gamma)}$), load-dependent components of Coulombic and viscous friction are constrained to zero value, thus equation (1) simplified to

$$\boldsymbol{T}_{\mathrm{fnl}(\gamma)} = -B_{(\gamma)} \cdot \boldsymbol{\omega}_{(\gamma)} + \boldsymbol{K}_{\mathrm{T}(\gamma)} I_{(\gamma)} \tag{2}$$

where the torque constant ($\boldsymbol{K}_{\mathrm{T}(\gamma)}$) of the motors are determined from handbooks, while angular velocity ($\boldsymbol{\omega}_{(\gamma)}$) and the motor currents ($I_{\mathrm{T}(\gamma)}$) are got from the I/O port of the machine tool and current sensors, respectively. The load-independent friction is linear by nature, therefore by plotting ($\boldsymbol{\omega}_{(\gamma)}$) against the value of product for ($\boldsymbol{K}_{\mathrm{T}(\gamma)}$) and ($I_{\mathrm{T}(\gamma)}$), then the load-independent Coulombic friction ($\boldsymbol{T}_{\mathrm{fnl}(\gamma)}$) is graphically determined as shown in Fig. 2. Then according to equation (2) and the determined values of $\boldsymbol{T}_{\mathrm{fnl}(\gamma)}$, damping coefficient of load-independent viscous friction ($B_{(\gamma)}$) is calculated. The results for the three-feed-systems of FA32M CNC Milling Machine from the procedure 1 are shown in Table 1.

Procedure 2. The signals of load-dependent components of Coulombic $\boldsymbol{T}_{\mathrm{Bf}(\gamma)}$ and viscous $\boldsymbol{T}_{\mathrm{fl}(\gamma)}$ frictions are all entangled with and also influenced by cutting force $\boldsymbol{T}_{\mathrm{cf}(\gamma)}$ signal. However, based on experimental investigations as demonstrated in graphs, the relationship between cutting torque ($\boldsymbol{T}_{\mathrm{cf}(\gamma)}$) and the total motor torque ($\boldsymbol{T}_{\mathrm{m}(x,y,z)}$) is largely linearly related. And

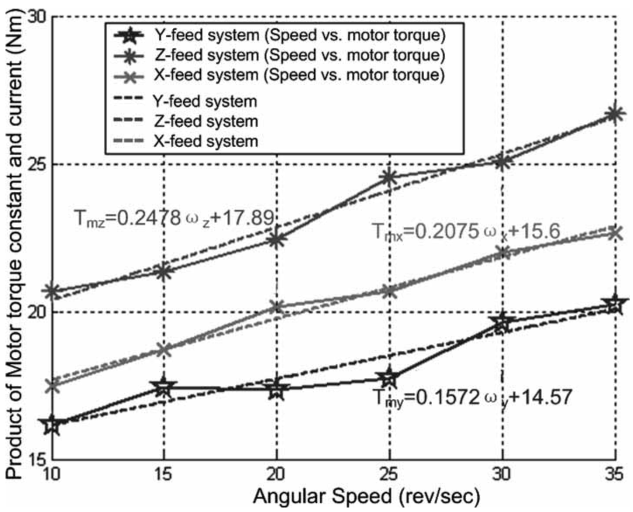

Fig. 2 Angular velocity versus total torque

Table 1 Results for the first procedure

Item	x feed system	y feed system	z feed system
$J_{(\gamma)}$	J_x/Nms^2 0.1471	J_y/Nms^2 0.1353	J_z/Nms^2 0.1569
$\boldsymbol{K}_{\mathrm{T}(\gamma)}$	$\boldsymbol{K}_{\mathrm{T}x}$/Kgf · m/A 15.878	$\boldsymbol{K}_{\mathrm{T}y}$/Kgf · m/A 15.878	$\boldsymbol{K}_{\mathrm{T}z}$/Kgf · m/A 15.878
$\boldsymbol{T}_{\mathrm{fnl}(\gamma)}$	$\boldsymbol{T}_{\mathrm{fnlx}}$/Nm 15.60	$\boldsymbol{T}_{\mathrm{fnly}}$/Nm 14.57	$\boldsymbol{T}_{\mathrm{fnlz}}$/Nm 17.89
$B_{(\gamma)}$	B_x/Nms/rev 0.2075	B_y/Nms/rev 0.1572	B_z/Nms/rev 0.2478

since the experiments were done at discrete and constant velocities, then the angular acceleration ($\boldsymbol{\varepsilon}_{(\gamma)}$) is constrained to zero value, consequently, the value of inertia torque is also zero. Based on this, deduction equation (1) is simplified as follows

$$\boldsymbol{K}_{\mathrm{T}(\gamma)} \cdot I_{\mathrm{T}(\gamma)} = B_{(\gamma)} \cdot \boldsymbol{\omega}_{(i)} + [\boldsymbol{T}_{\mathrm{fnl}(\gamma)} + (\boldsymbol{T}_{\mathrm{fl}(\gamma)} + \boldsymbol{T}_{\mathrm{Bf}(\gamma)}) + \boldsymbol{T}_{\mathrm{cf}(\gamma)}] \tag{3}$$

Based on the fact that cutting force is directly and directly proportional to motor torque, then the resultants of load-dependent components of coulombic and viscous frictions are also directly proportional to cutting force. Then all the cutting force-dependent variables in equation (3) are expressed as a function of cutting force torque

$$\boldsymbol{K}_{\mathrm{T}(\gamma)} \cdot I_{\mathrm{T}(\gamma)} = B_{(\gamma)} \cdot \boldsymbol{\omega}_{(\gamma)} + \boldsymbol{T}_{\mathrm{fnl}(\gamma)} + [\boldsymbol{T}_{\mathrm{cf}(\gamma)} + f(\boldsymbol{T}_{\mathrm{cf}(\gamma)})] \tag{4}$$

where $f(\boldsymbol{T}_{\mathrm{cf}(\gamma)})$ is a function of cutting force.

As already deduced, that cutting force is proportional to motor torque, then a constant ($K_{\mathrm{BLf}(\gamma)}$) is introduced, then

$$f(\boldsymbol{T}_{\mathrm{cf}(\gamma)}) = \boldsymbol{T}_{\mathrm{cf}(\gamma)} + \boldsymbol{T}_{\mathrm{cf}(\gamma)} K_{\mathrm{BLf}(\gamma)} \tag{5}$$

Combining equations (4) and (5) is simplified then

$$\boldsymbol{K}_{\mathrm{T}(\gamma)} \cdot I_{\mathrm{T}(\gamma)} = B_{(\gamma)} \cdot \boldsymbol{\omega}_{(\gamma)} + \boldsymbol{T}_{\mathrm{fnl}(\gamma)} + \boldsymbol{T}_{\mathrm{cf}(\gamma)} K_{\mathrm{BLf}(\gamma)} \tag{6}$$

As illustrated in Fig. 3, the friction load factor ($K_{\mathrm{BLf}(i)}$) for x, y, and z feed systems (K_{BLfx}, K_{BLfy}, and K_{BLfz}) are determined using graphical regression analysis as 0.006 25, 0.005 81, and 0.003 89, respectively.

Then equation (1) is updated to

$$\left.\begin{aligned} \boldsymbol{\varepsilon}_x &= 107.9 \cdot I_{\mathrm{T}x} - 13.83 \cdot \boldsymbol{\omega}_x - 0.417 \cdot \boldsymbol{T}_{\mathrm{cfx}} - 1040 \\ \boldsymbol{\varepsilon}_y &= 117.3 \cdot I_{\mathrm{T}y} - 11.39 \cdot \boldsymbol{\omega}_y - 0.421 \cdot \boldsymbol{T}_{\mathrm{cfy}} - 1056 \\ \boldsymbol{\varepsilon}_z &= 101.2 \cdot I_{\mathrm{T}z} - 15.49 \cdot \boldsymbol{\omega}_z - 0.243 \cdot \boldsymbol{T}_{\mathrm{cfz}} - 1118 \end{aligned}\right\} \tag{7}$$

for all the three-feed systems. Consequently, this marks the accomplishment of task for establishing

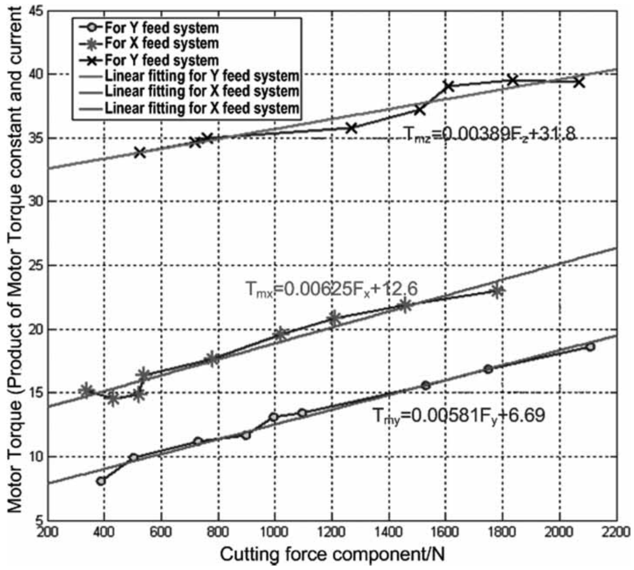

Fig. 3 Motor torque versus force dynamometer reading

the relationship between the cutting forces and motor current.

The proceeding task is to establish the relationship between cutting force and motor current. Auspiciously, values of the corresponding induced errors corresponding to the cutting forces were established by position sensors in procedure 2. By graphical regression analysis, the predominantly linear relationship (see Fig. 4) between cutting force and the cutting force induced errors is established as follows

$$\left.\begin{aligned}\boldsymbol{\delta}_x &= 0.007\,43 \cdot \boldsymbol{T}_{\text{cfx}}\\ \boldsymbol{\delta}_y &= 0.005\,41 \cdot \boldsymbol{T}_{\text{cfy}}\\ \boldsymbol{\delta}_z &= 0.002\,46 \cdot \boldsymbol{T}_{\text{cfz}}\end{aligned}\right\} \tag{8}$$

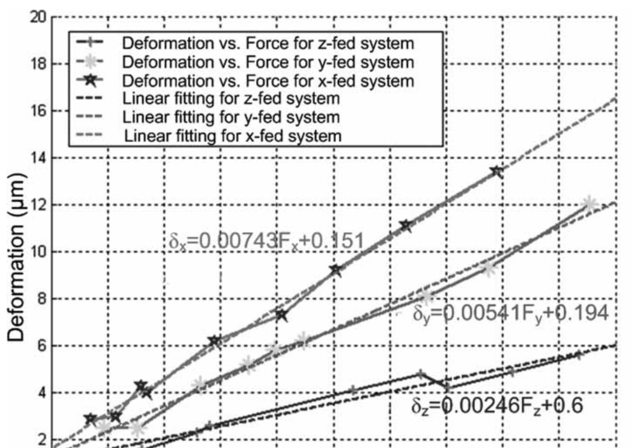

Fig. 4 Cutting force versus total machine deformation

Combining and simplifying equations (7) and (8) gives

$$\left.\begin{aligned}\boldsymbol{\delta}_x &= 1.925 \cdot I_{\text{Tx}} - 0.247 \cdot \boldsymbol{\omega}_x - 0.0178 \cdot \boldsymbol{\varepsilon}_x - 18.545\\ \boldsymbol{\delta}_y &= 1.508 \cdot I_{\text{Ty}} - 0.146 \cdot \boldsymbol{\omega}_y - 0.0128 \cdot \boldsymbol{\varepsilon}_y - 13.567\\ \boldsymbol{\delta}_z &= 1.024 \cdot I_{\text{Tz}} - 0.157 \cdot \boldsymbol{\omega}_z - 0.0101 \cdot \boldsymbol{\varepsilon}_z - 11.314\end{aligned}\right\} \tag{9}$$

The cutting force induced errors components are expressed as a function of motor current, angular velocity, and angular acceleration

$$\boldsymbol{\delta}_{(x,y,z)} = f(I_{\text{T}(x,y,z)}, \boldsymbol{\omega}_{(x,y,z)}, \boldsymbol{\varepsilon}_{(x,y,z)}) \tag{10}$$

and indicating that the cutting force variable is eliminated. This means that the cutting force signal is not required and therefore, the force dynamometer is no longer necessary.

The compensation systems is provided with data from the machine parameters (angular velocity, angular acceleration) from the CNC machine I/O port and motor current from online Hall effect current sensors. Finally, based on this values and in accordance with equation (9), cutting force-induced error is determined in real-time.

3 SYNTHESIS MODEL FOR THE CUTTING FORCE ERROR

The system monitors the cutting force induced errors individually according to respective feed systems. However, the compensation of cutting forces is accomplished by a single model on a single board. Based on this reason, all cutting force induced errors are compounded into one synthesis model. Each and every error component is propagated from its local coordinate systems till the absolute coordinate system of the machine tool using homogenous transformation method [**2**].

In the synthesis modelling, the necessary condition for traditional machining processes taking place is that on the cutting tool and workpiece must touch is followed. Meaning that, cutting and being-point(s) on the cutting and workpiece, respectively, are at same absolute spatial location. Furthermore, the tool and workpiece systems on same machine tool share the same absolute frame. Therefore, if touching points on the tool and workpiece are transformed to absolute coordinate system, their the coordinates are equal, then

$$\begin{aligned}&\boldsymbol{\tau}^{i+1}_{i(\gamma)}\boldsymbol{\tau}^{i+2}_{i+1(\gamma)}\cdots\boldsymbol{\tau}^{n}_{n-1(\gamma)}(\boldsymbol{W}_{(\gamma)} + \boldsymbol{\Delta}_{(\gamma)})_m\\ &\quad = \boldsymbol{\tau}^{j+1}_{j(\gamma)}\boldsymbol{\tau}^{j+2}_{j+1(\gamma)}\cdots\boldsymbol{\tau}^{m}_{m-1(\gamma)}(\boldsymbol{T}_{(\gamma)})_n \quad (i = 1, 2, \ldots, m);\\ &\qquad (j = 1, 2, \ldots, n)\end{aligned} \tag{11}$$

where m and n are number of frames in the workpiece and the tool system, respectively.

The three-axis FA 32M CNC milling machine has one frame (D) in the tool system and two frames (B and C) in the workpiece system, implying that $m = 2$ while $n = 1$, hence

$$\boldsymbol{\tau}^{B}_{A(\gamma)}\boldsymbol{\tau}^{C}_{B(\gamma)}(\boldsymbol{W}_{C(\gamma)} + \boldsymbol{\Delta}_{(\gamma)})_m = \boldsymbol{\tau}^{D}_{A(\gamma)}(\boldsymbol{T}_{D(\gamma)})_n \tag{12}$$

According to equation (9) and on the basis of the details for positions of respective frames as per CNC controller, the values of error as per online sensor, the synthesis model is then determined. Finally, according to equation (12), based on respective frame positions and current values, volumetric error is determined in real-time.

4 COMPENSATION SYSTEM AND ITS EVALUATION

The proposed compensation system for cutting force-induced error is achieved through both hardware and software environments.

4.1 Hardware

As illustrated in Fig. 5, the multi-purpose compensator is specifically composed of single chip microcomputer (SCM) system, power module; RS232 serial communication module; I/O 8255 expansion module and programmable controller (PMC). The compensation process starts by reading the induced current values from the online Hall effect sensor. Then the current signal is conditioned (A/D conversion and filtration) and then interpreted by the compensation model embedded in the ROM of the SCM.

Through the periodic scan of B2 I/O port by the ladder program in the PMC, the current digital signal and the external machine data are dispatched to the CNC controller. Finally the CNC controller effects the compensation utilizing the inherent function of external shifting of the origins of coordinate systems.

4.2 Software

Software in this system is responsible for representation of compensation model, creating the computer interface and data interfacing. The model is written using the C51 compiler whereas the computer interface is written using MS Visual Basic 6.0. Data interfacing is accomplished by utilizing the RS232 ActiveX module of MS Visual Basic 6.0. Data interfacing accomplishes the function of model embedding and communication between the personal computer, compensator, and CNC controller.

4.3 Evaluation

In order to evaluate the performance of compensation system, a series of machining tests were conducted using a milling tool and machining parameter (depth of cut, cutting speed). A six pair of 'L' form groves were machined into carbon steel workpiece with a series of different depths of cuts. Carbon steel workpieces of hardness 30 HRC and tungsten carbide (10 per cent cobalt content) milling tool were used. The milling parameters are 2.0 mm of tool diameter, 4000 rpm of angular speed and 400 mm/min of feed speed. One of each pair of grooves with same depth of cut was machined with and the other without engagement of compensation system. Finally, post-inspection of the workpieces was conducted using the three-dimensional laser coordinate measuring machine. As shown in Fig. 6, the comparison of

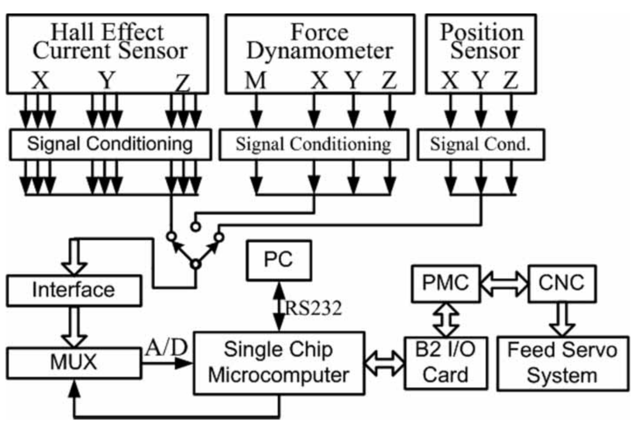

Fig. 5 Compensator hardware configuration

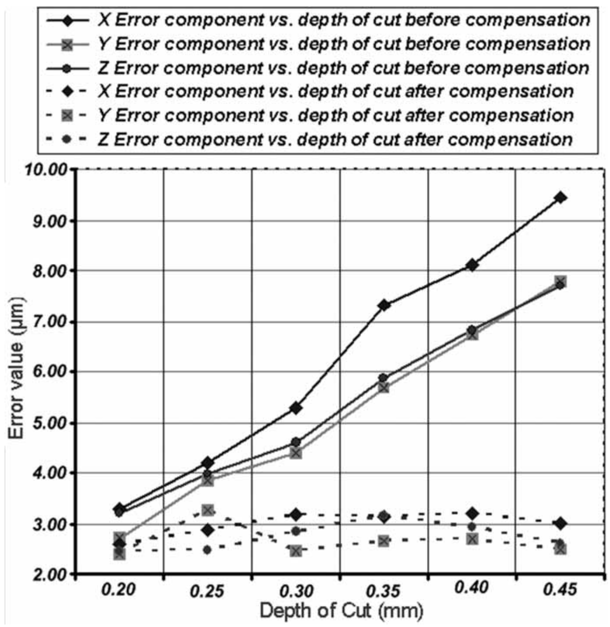

Fig. 6 Systems evaluation results

accuracy of the workpiece with and without compensation demonstrates the system's capacity for improving the machining accuracy.

5 CONCLUSION

The current paper presented a precise real-time compensation system for force-induced error on three-axis CNC Miller with comprehensive account of frictional loads. An optimally economical and convenient system was developed based on indirect monitoring of motor current by Hall effect current sensor. Strategic parallel running of calibration and modelling data acquisition has proved to be a very effective and efficient in this procedure. A wide range of possibilities for accurate modelling of complex phenomena in the machine tool kinematic chain were provided. Ultimately, a precise and cost effective compensation system for cutting force-induced error was achieved.

REFERENCES

1 **Sutton, G. P.** Economy of accuracy. In *Technology of machine tools, vol. 5: machine tool accuracy* (Ed. R. Hocken), 1980 (Lawrence Livermore National Laboratories, University of California, Livermore, CA).

2 **Ramesh, R., Manna, M. A.,** and **Poo, A. N.** Error compensation in machine tools – a review part I: geometric, cutting-force induced and fixture dependent errors. *Int. J. Mach. Tools Manuf.*, 2000, **40**, 1235–1256.

3 **Okafor, A. C.** and **Ertekin, Y. M.** Derivation of machine tool error models and error compensation procedure for three axes vertical center using rigid body kinematics. *Int. J. Mach. Tools Manuf.*, 2000, **40**, 1199–1213.

4 **Koren, Y.** and **Masory, O.** Adaptive control with process estimation. *Ann. CIRP*, 1981, **30**, 373–376.

5 **Ulsoy, A. G.** and **Koren, Y.,** Applications of adaptive control to machine tool process control. *IEEE Control Syst. Mag.*, 1989, **9**, 33–37.

6 **Huang, Y.** and **Liang, S. Y.** Cutting forces modeling considering the effect of tool thermal property-application to CBN hard turning. *Int. J. Mach. Tools Manuf.*, 2003, **43**, 307–315.

7 **Endres, W., Sutherland, J., Devor, R.,** and **Kapoor, S.** A dynamic model of the cutting force system in the turning process. In *Monitoring and control for manufacturing process*, vol. 44, pp. 193–212 (ASME PED, ASME, New York).

8 **Li, X., Venuvinod, P. K.,** and **Chen, M. K.** Feed cutting force estimation from the current measurement with hybrid learning. *Int. J. Adv. Manuf. Technol.*, 2000, **16**, 859–862.

9 **Stein, J. L.** and **Huh, K.** Monitoring cutting forces in turning – a model-based approach. *Trans. ASME*, 2000, **124**, 30.

10 **Kim, T.** and **Kim, J.** Adaptive cutting force control for a machining center by using indirect cutting force measurements. *Int. J. Mach. Tools Manuf.*, 1996, **36**, 925–937.

11 **Saraie, H., Sakahira, M., Ibaraki, S., Matsubara, A., Kakino, Y.,** and **Fujishima, M.** Monitoring and adaptive control of cutting forces based on spindle motor currents in machining centers. In Proceedings of the 2nd International Conference of LEM21, Niigata, Japan, November 2003, pp. 555–560.

APPENDIX

Notation

$B_{(x,y,z)}$	x, y, or z components damping coefficient of load independent viscous friction
$\boldsymbol{F}_{(x,y,z)}$	x, y, or z components of cutting force as seen by the force dynamometer
$J_{(x,y,z)}$	moment of inertia for kinematic chain of x, y, or z servo system
$K_{\mathrm{BLf}(x,y,z)}$	friction load factor for kinematic chain of x, y, or z servo system
$\boldsymbol{K}_{\mathrm{T}(x,y,z)}$	motor torque coefficient for drive motor of x, y, or z servo system
$\boldsymbol{T}_{\mathrm{D}(x,y,z)}$	x, y, or z components of position vector for cutting tool tip in the local frame (D)
$\boldsymbol{T}_{\mathrm{Bf}(x,y,z)}$	x, y, or z components of viscous friction torque increase due to cutting load
$\boldsymbol{T}_{\mathrm{cf}(x,y,z)}$	x, y, or z components of cutting force torque
$\boldsymbol{T}_{\mathrm{fl}(x,y,z)}$	x, y, or z components of Coulombic friction torque increase due to cutting load
$\boldsymbol{T}_{\mathrm{fnl}(x,y,z)}$	x, y, or z components of Coulombic friction torque independent from loading
$\boldsymbol{T}_{\mathrm{m}(x,y,z)}$	x, y, or z components of torque is as seen by the motor
$\boldsymbol{W}_{\mathrm{C}(x,y,z)}$	x, y, or z components of position vector for the workpiece in the local frame (C)
γ	stands for (x, y, z)
$\boldsymbol{\delta}_{(x,y,z)}$	x, y, or z components of machine tool deformation
$\boldsymbol{\Delta}_{(x,y,z)}$	x, y, or z components of workpiece error
$\boldsymbol{\varepsilon}_{(x,y,z)}$	x, y, or z components of angular acceleration
$\boldsymbol{\tau}^{i+1}_{i(x,y,z)}$	x, y, or z components of transformation matrix from $i+1$ to workpiece i frame
$\boldsymbol{\tau}^{j+1}_{j(x,y,z)}$	x, y, or z components of transformation matrix from $j+1$ to wheel j frame
$\boldsymbol{\omega}_{(x,y,z)}$	x, y, or z components of angular velocity